JOURNAL OF VIROLOGY, Oct. 1993, p. 6015–6024
0022-538X/93/106015-10$02.00/0

Vol. 67, No. 10

Intracerebral Hemorrhages and Syncytium Formation Induced by Endothelial Cell Infection with a Murine Leukemia Virus

BEN HO PARK,[1] EHUD LAVI,[2] KENNETH J. BLANK,[3] AND GLEN N. GAULTON[1]*

Department of Pathology and Laboratory Medicine, Division of Immunobiology,[1] and Division of Neuropathology,[2] University of Pennsylvania, Philadelphia, Pennsylvania 19104, and Department of Pathology, Hahnemann University School of Medicine, Philadelphia, Pennsylvania 19102[3]

Received 25 February 1993/Accepted 30 June 1993

The mechanisms of endothelial cell damage that lead to cerebral hemorrhage are not completely understood. In this study, a cloned murine retrovirus, TR1.3, that uniformly induced stroke in neonatal BALB/c mice is described. Restriction digest mapping suggests that TR1.3 is part of the Friend murine leukemia virus (FMuLV) family. However, unlike mice exposed to other FMuLVs, mice infected with TR1.3 virus developed tremors and seizures within 8 to 18 days postinoculation. This was uniformly followed by paralysis and death within 1 to 2 days. Postmortem examination of TR1.3-inoculated mice revealed edematous brain tissue with large areas of intracerebral hemorrhage. Histologic analysis revealed prominent small vessel pathology including syncytium formation of endothelial cells. Immunohistochemical analysis of frozen brain sections using double fluorescence staining demonstrated that TR1.3 virus specifically infected small vessel endothelial cells. Although infection of vessel endothelial cells was detected in several organs, only brain endothelial cells displayed viral infection associated with hemorrhage. The primary determinant of TR1.3-induced neuropathogenicity was found to reside within a 3.0-kb fragment containing the 3′ end of the *pol* gene, the *env* gene, and the U3 region of the long terminal repeat. The restricted tropism and acute pathogenicity of this cloned murine retrovirus provide a model for studying virus-induced stroke and for elucidating the mechanisms involved in syncytium formation by retroviruses in vivo.

Endothelial cell damage is believed to be an essential factor in the initiation of a cascade of pathologic processes leading to the clinical symptoms of stroke (28). Several investigations suggest that viral infection of endothelial cells may trigger this process (2, 9). For example, an increased frequency of stroke has been described in patients infected with varicella-zoster virus (27, 32) and human immunodeficiency virus type 1 (3, 8). Human immunodeficiency virus type 1 has been detected in brain capillary endothelial cells (CEC) of some AIDS patients (38), and it is postulated that retroviral infection of brain CEC may lead to the rupture and occlusion of vessel walls (30).

A number of mouse retroviruses within the murine leukemia virus (MuLV) family have been shown to induce central nervous system (CNS) pathology when inoculated into susceptible strains of neonatal mice. These MuLVs infect neuronal (31), glial (18), and endothelial (23) cells and may induce noninflammatory changes in the anterior lateral horns of the lumbosacral spinal cord with reactive gliosis and neuronal death (11). However, no studies have demonstrated that MuLV-induced endothelial cell pathology leads directly to neurodegenerative changes.

Virus variants derived from T-cell tropic MuLV exhibit specific patterns of CNS infection (33). The neurotropism of one such variant, TR1.3, was assessed. TR1.3 is an infectious MuLV derived from a molecular clone, E55+, that was isolated from the leukemic T-cell line Kgv (36). Neonatal (<24 h old) BALB/c mice that were inoculated with TR1.3 uniformly developed tremors and seizure by 8 to 18 days. Autopsy of diseased mice showed edematous brain tissue, accompanied by large hemorrhagic areas. Microscopic examination of these brains verified the presence of erythrocytes exiting vessels and extravasated into the brain parenchyma. Numerous examples of syncytium formation of cerebral vessel endothelial cells were also observed. Immunohistochemical analysis of serial sections indicated that the TR1.3 virus specifically infected vessel endothelial cells at the sites of vessel dysfunction. The primary determinant of TR1.3's neuropathogenicity was mapped by using recombinant viruses and was found to reside within a 3.0-kb fragment containing the 3′ portion of the *pol* gene, the entire *env* gene, and the U3 region of the long terminal repeat (LTR). The relevance of these observations to retrovirus-induced stroke is discussed.

MATERIALS AND METHODS

Mice. Virus-free pregnant female BALB/c mice were obtained from Charles River (Wilmington, Mass.). Mice were monitored daily for birth of litters. Newborn litters were used within the first 24 h after birth for inoculations by either the intracerebral (i.c.) or the intraperitoneal (i.p.) route. Mice were maintained on standard laboratory food and water ad libitum.

Viruses. A molecular clone of the Friend MuLV (FMuLV) FB29 was used for comparative restriction analysis (34). FB29 was cloned at its unique *Hin*dIII site by using the modified vector pUC19B. Derivation of the ecotropic molecular clone E55+ has been described elsewhere (36). Briefly, this molecular clone was isolated from the T-cell leukemic line Kgv. Kgv was itself isolated from the lymphoid tissue of mice infected with Gross Passage A MuLV (13). E55+ was cloned into the *Eco*RI site of pBluescript (Stratagene, La Jolla, Calif.) by the methods of Hirt (15). For restriction digest mapping and construction of recombinant viruses, E55+ was subcloned at its unique *Hin*dIII site into

* Corresponding author.

the pUC19B vector in the same orientation as FB29 and renamed TR1.3.

Plasmids FB29 and TR1.3 were used to generate the recombinant viruses R3.5 and R4.3. FB29 and TR1.3 plasmid DNAs were digested with *Sph*I and *Asc*I, and complementary fragments were ligated with T4 DNA ligase (Boehringer Mannheim Biochemicals, Indianapolis, Ind.) overnight at 16°C. The recombinant viruses were transformed in bacteria, screened by restriction digest analysis, and used for generating infectious virus.

Infectious virus was produced by gel isolation of the permuted viruses from pUC19B after digestion with *Hin*dIII. Virus was then circularized with T4 DNA ligase and transfected into the feral mouse embryo fibroblast cell line, Sc-1 (American Type Culture Collection, Rockville, Md.), as described elsewhere (37). After 10 days in culture, supernatants were harvested and assayed for the presence of reverse transcriptase (RT) (12). Viral supernatants were aliquoted and stored at −70°C. Viral titers were determined by a modified XC cell plaque assay (29). Supernatant from mock-transfected Sc-1 cells was used as a control in all subsequent in vivo experiments. Sc-1 cells were grown in minimal essential medium supplemented with 10% fetal calf serum and 1% penicillin and streptomycin.

Inoculations. Neonates were injected either i.c. with 1.5×10^3 PFU or i.p. with 3×10^3 PFU of TR1.3 viral supernatants within the first 24 h after birth. Control mice were inoculated with an equal volume of supernatant from mock-transfected Sc-1 cells. Mice were monitored daily for symptoms of tremor, seizure, and paralysis. For recombinant virus studies, equal amounts of titers of the viruses TR1.3, FB29, R3.5, and R4.3, as assessed by the RT assay, were injected i.c. into neonatal BALB/c mice within the first 24 h after birth.

Primary CNS cultures. TR1.3-infected animals and age-matched mock-infected controls were euthanized at the first sign of neurologic disease. Whole brains were dissected and minced into 1-mm^3 fragments and adapted to 75-cm^2 tissue culture flasks. Primary cultures were grown for 1 week in minimal essential medium supplemented with 10% fetal calf serum and 1% penicillin and streptomycin (33).

Antibodies and lectin. Purified polyclonal goat anti-Rauscher gp70 was obtained from the Biological Carcinogenesis branch of the National Cancer Institute (Bethesda, Md.). Fluorescein-conjugated monoclonal rat anti-goat immunoglobulin G was purchased from Fisher Scientific Co. (Pittsburgh, Pa.). Rhodamine-conjugated BS-1 lectin was purchased from Sigma Chemical Co. (St. Louis, Mo.).

Immunohistochemical analyses. Frozen tissue sections were prepared from brains, kidneys, and livers of 2-week-old mice that had been inoculated with TR1.3 virus or from age-matched mock-infected controls. Serial sections 6 μm thick were fixed with methanol for 2 min at −20°C and then incubated with normal sheep serum (2% in 20 mM sodium phosphate [pH 7.4]–150 mM sodium chloride [PBS]) for 20 min at 4°C. Sections were then incubated with primary antibodies, and then fluorescein- and rhodamine-conjugated secondary reagents were added for 30 min at 4°C. Three washes in PBS were performed on each section between incubations. Goat anti-Rauscher gp70 antibody and fluorescein isothiocyanate-conjugated rat anti-goat immunoglobulin G were used at final concentrations of 95 and 5 μg/ml, respectively. BS-1 lectin was used at a final concentration of 50 μg/ml. Sections were analyzed with a Nikon Optiphot fluorescence microscope.

Histopathological analyses. Tissue samples from brains, lungs, livers, spleens, and kidneys were taken from 2-week-old mice that were inoculated with TR1.3 virus or from age-matched mock-infected controls. Organs were fixed in formalin and embedded in paraffin, and serial sections were prepared for hematoxylin and eosin staining.

TABLE 1. Onset of neurologic disease in neonatal BALB/c mice infected with TR1.3 MuLV

Experiment no.	No. of diseased mice/ no. in group[a]	Time (days) to onset of disease[b]	Inoculation route[c]
1	5/5	8–9	i.c.
2	3/3	8–9	i.c.
3	4/4	11–12	i.c.
4	7/7	11–12	i.c.
5	3/3	12–13	i.c.
6	4/4	10–12	i.c.
7	4/4	12–18	i.p.
8	5/5	12–16	i.p.

[a] All mice died within 1 to 2 days following the onset of disease, except those mice that were sacrificed for histologic analyses.

[b] Onset of disease was judged as the first day on which mice displayed symptoms of tremors or seizures. The interval describes when the first and last mouse of the litter, respectively, developed disease.

[c] All injections were done with neonatal BALB/c mice within 24 h after birth. 1.5×10^3 and 3×10^3 PFU of TR1.3 viral supernatant were used for i.c. and i.p. inoculations, respectively.

Electron microscopy. Diseased mice were anesthetized with ether and perfused through the left ventricle with a fixative solution of 4% paraformaldehyde and 2% glutaraldehyde in 0.1 M cacodylate buffer, pH 7.35. The brains were dissected intact and then cut into 1-mm^3 fragments. The tissues were washed, postfixed in 1% osmium tetroxide–1.5% potassium ferrocyanide, dehydrated in ethanol, and embedded in Araldite. Sections were embedded flat and cross-sectioned to determine areas appropriate for evaluation. Selected regions were thin-sectioned (8- to 10-μm-thick sections) on an LKB ultramicrotome, stained with aqueous uranyl acetate and lead citrate, and viewed by a transmission electron microscope (100CX; JEOL).

RESULTS

TR1.3-induced neurologic disease and death in neonatal mice. The neurotropic and neuropathogenic effects of TR1.3 virus were examined following i.p. or i.c. inoculation of neonatal BALB/c mice (<24 h old). As shown in Table 1, mice developed tremors and seizure activity 8 to 18 days postinoculation. This was uniformly followed by paralysis and death within 1 to 2 days after the onset of neurologic symptoms. CNS disease occurred in 100% of mice tested and was observed in 35 mice over eight separate experiments. Mock-infected mice remained healthy and did not display any neurologic abnormalities. Postmortem examination of TR1.3-inoculated mice revealed multiple foci of hemorrhagic lesions throughout the brain (Fig. 1). In addition, the brains were significantly more edematous than those of mock-infected age-matched controls. Hemorrhages were present in brain tissue but not in liver, lung, heart, kidney, or spleen tissue of mice inoculated with TR1.3 by either an i.p. or an i.c. route.

TR1.3 infects vessel endothelial cells. The cellular location of TR1.3 infection within the CNS was determined by immunofluorescence analysis of frozen brain sections. The presence of virus was determined by binding of a polyclonal goat anti-MuLV gp70 antibody that recognizes the gp70 viral envelope protein of MuLV and visualized with a secondary

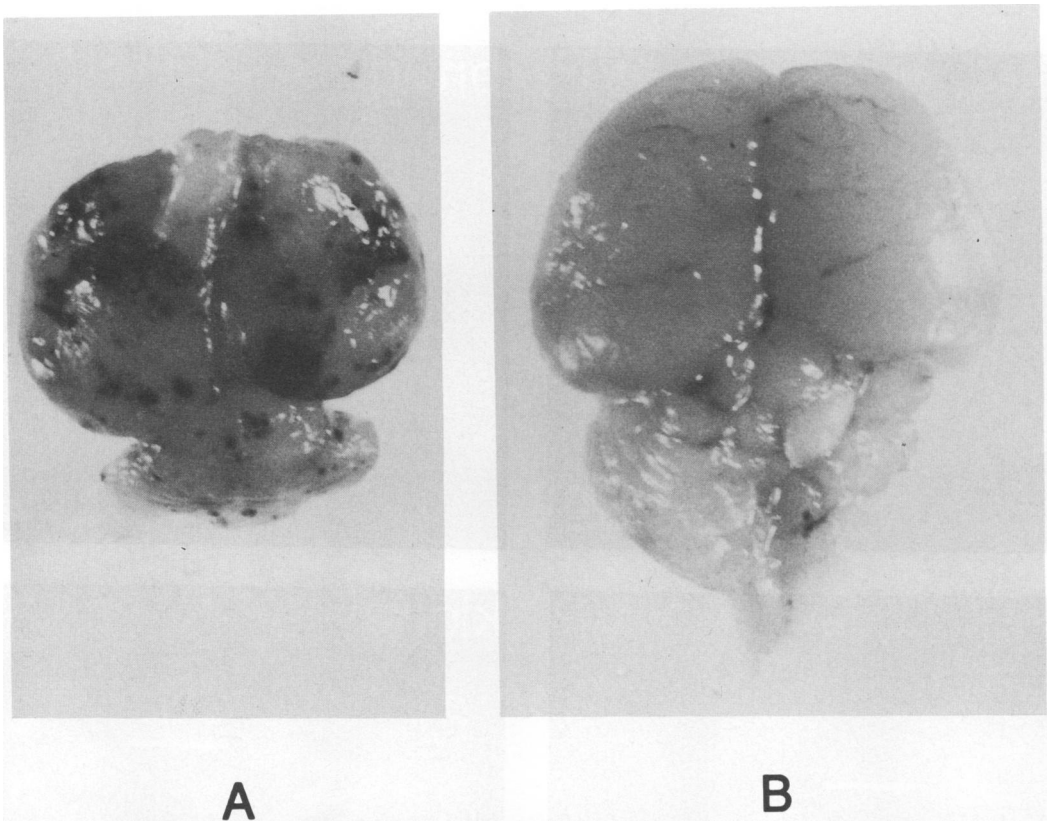

FIG. 1. Neonatal BALB/c mice infected with TR1.3 develop i.c. hemorrhages. Neonatal BALB/c mice (<24 h old) were injected i.c. with either TR1.3 virus (A) or mock-transfected supernatant (B). Animals displaying neurologic symptoms and age-matched mock-infected controls were euthanized immediately. The brains from these mice were dissected, fixed in formalin, and photographed.

fluorescein isothiocyanate-labeled anti-goat reagent. The location of endothelial cells was determined by binding of a tetramethyl rhodamine isothiocyanate-labeled lectin, BS-1, that selectively recognizes murine endothelial cells (17). A comparison of the viral protein and endothelial cell staining patterns shown in Fig. 2 revealed that viral infection was exclusively localized to vessel endothelial cells in the brain (top panel). Mock-infected controls were uniformly negative for viral gp70 expression (data not shown). Similar analysis also identified virus infection within endothelial cells of other organs such as the kidneys (Fig. 2, middle panel) and the liver (bottom panel). Interestingly, the majority of liver sinusoidal endothelium that stained with the BS-1 lectin did not stain for viral protein expression, indicating the TR1.3 virus preferentially infects vessel endothelium (Fig. 2, bottom panel).

Microscopic pathology in TR1.3-infected brains. Hematoxylin-and-eosin-stained sections were prepared from the brains of symptomatic TR1.3-infected mice to visualize the pathologic processes in these animals. Analysis of infected brain tissue under low magnification (Fig. 3A) demonstrated multiple areas of cerebral hemorrhage, which correlates with the gross pathology shown in Fig. 1. Examination under higher magnification revealed erythrocytes that were extravasated into the brain tissue through damaged vessel walls (Fig. 3B). Cerebral blood vessels exhibited various degrees of pathology ranging from mild cellular changes of endothelial cells to overt necrosis with hemorrhage. Although the kidneys and livers of TR1.3-infected mice also demonstrated viral infection as detected by double fluorescence staining, no gross or microscopic areas of hemorrhage were observed in these organs and there was no evidence of endothelial cell pathology on histologic examination (Fig. 3C and D).

The presence of brain endothelial cells with abnormal morphology was detected by high magnification of both double fluorescence- and hematoxylin-and-eosin-stained sections. Histologic analysis revealed multinucleated giant cells lining the vessel lumen, suggesting that these abnormal cells were the result of syncytium formation of cerebral vessel endothelial cells (Fig. 4A). The identification of these multinucleated cells and the presence of viral infection were verified by double fluorescence staining. As shown in Fig. 4B, there was complete colocalization of anti-gp70 and BS-1 lectin staining in these multinucleated cells. The presence of morphologically abnormal endothelial cells with multiple nuclei was confirmed by electron microscopy (Fig. 4C). Syncytia were often seen with necrosed vessels and were found throughout the brain in both grey and white matter; however, not all infected endothelial cells within the brain displayed syncytium formation.

Isolation of virus from TR1.3-infected mice. The infectious component of this response was confirmed by in vitro primary tissue culture of brain tissue from mock-infected and TR1.3-infected mice. After 1 week in culture, supernatants were harvested and the production of retrovirus was assayed by the presence of RT. Culture supernatants from infected brain tissues displayed RT activity, while culture supernatants from mock-infected brains showed no RT activity (data not shown). RT-positive supernatants from these cultures were then used to reinfect neonatal BALB/c

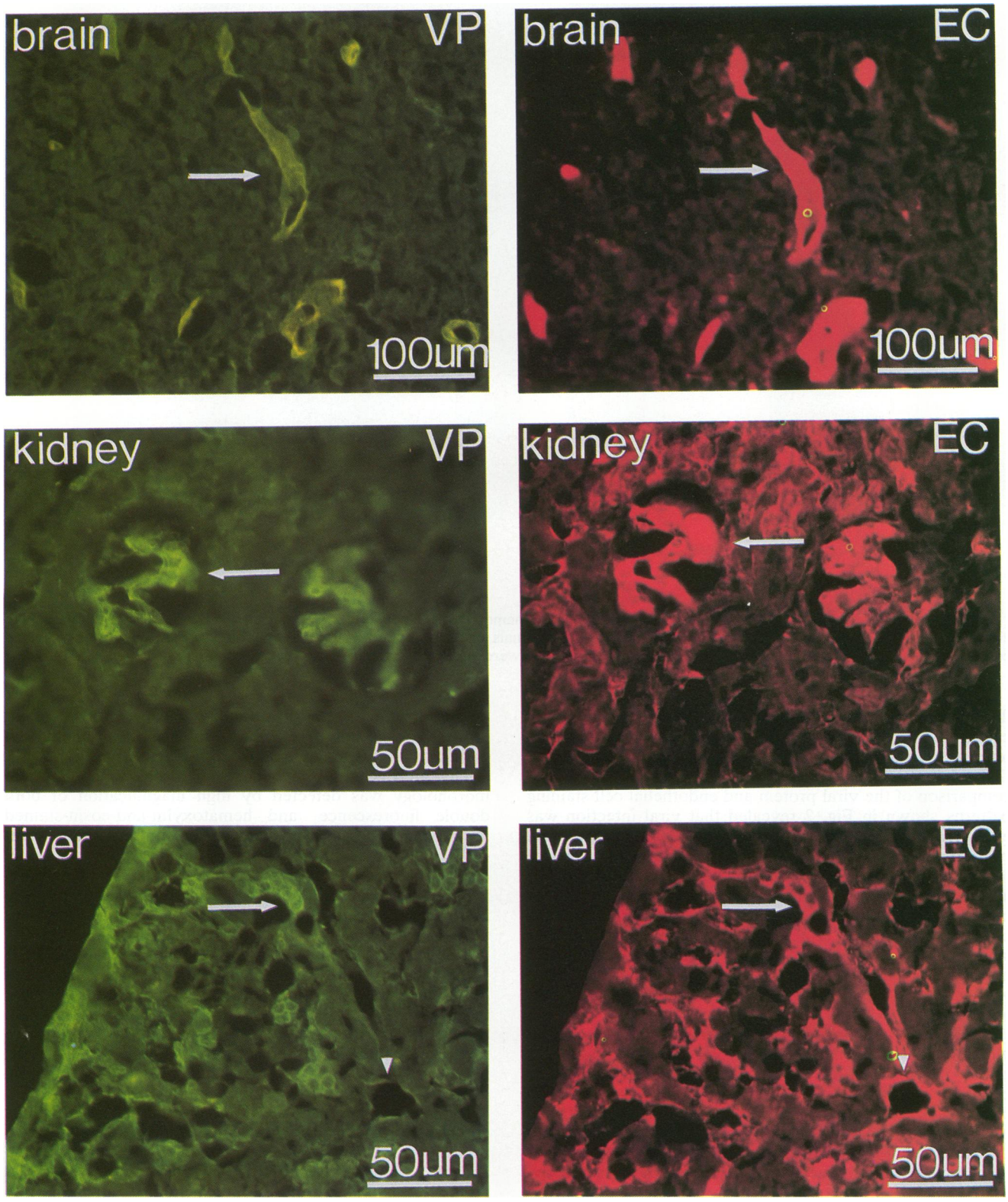

FIG. 2. TR1.3 infects capillary endothelial cells. Double positive staining of frozen sections with anti-Rauscher gp70 antibody to detect viral protein (VP) and BS-1 lectin to detect endothelial cells (EC) within the brains, kidneys, and livers of TR1.3-infected mice is shown. Arrows denote staining with both antibody and lectin, and arrowheads denote staining with lectin only.

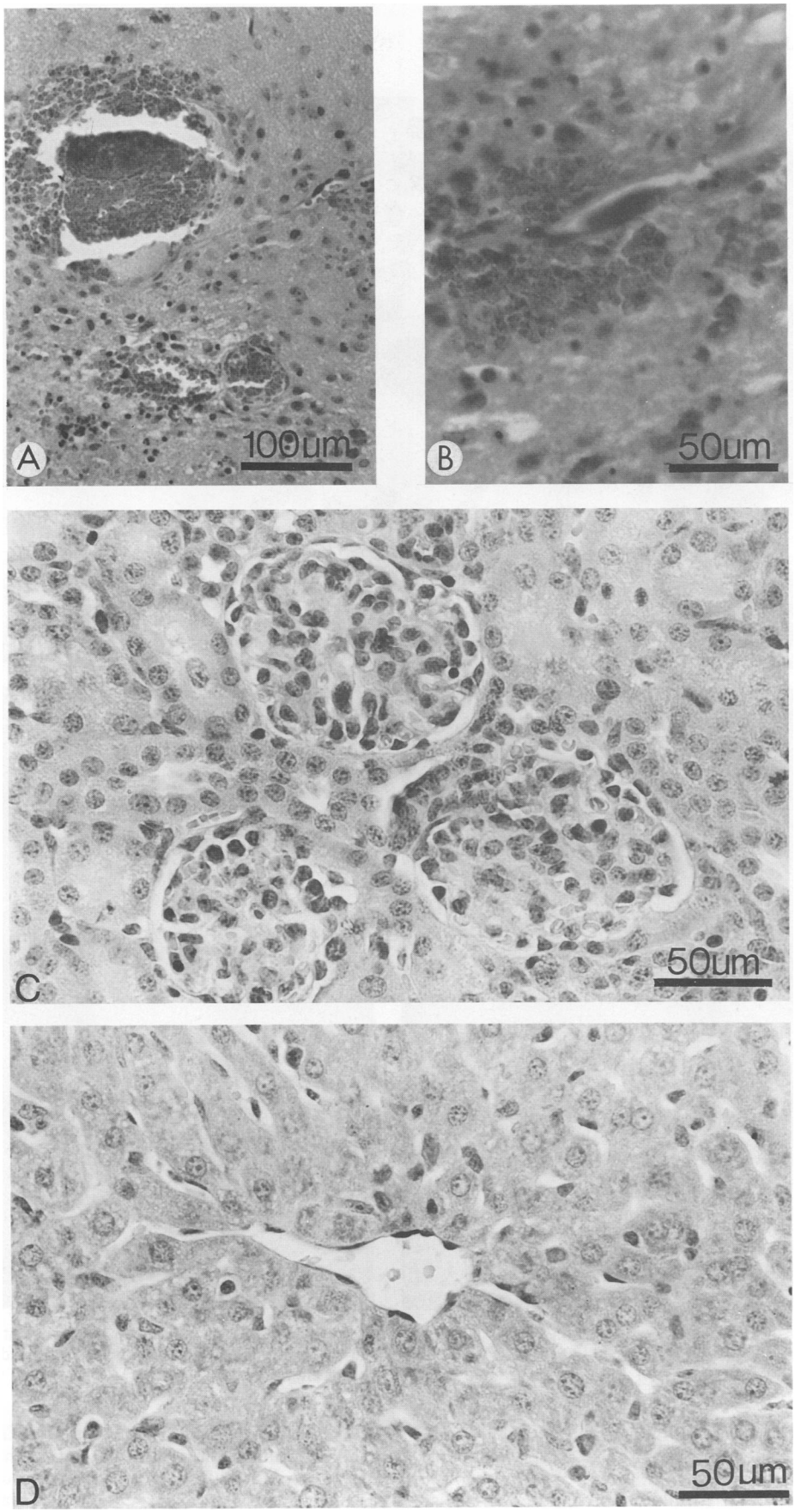

FIG. 3. Hematoxylin-and-eosin-stained sections from TR1.3-infected mice. (A and B) Brain. A low-power view of multiple hemorrhagic areas and a high-power view of erythrocytes exiting the vessel lumen are shown, respectively. (C) Kidney. A high-power view of cortical glomeruli is shown. (D) Liver. A high-power view of hepatocytes and the central vein is shown.

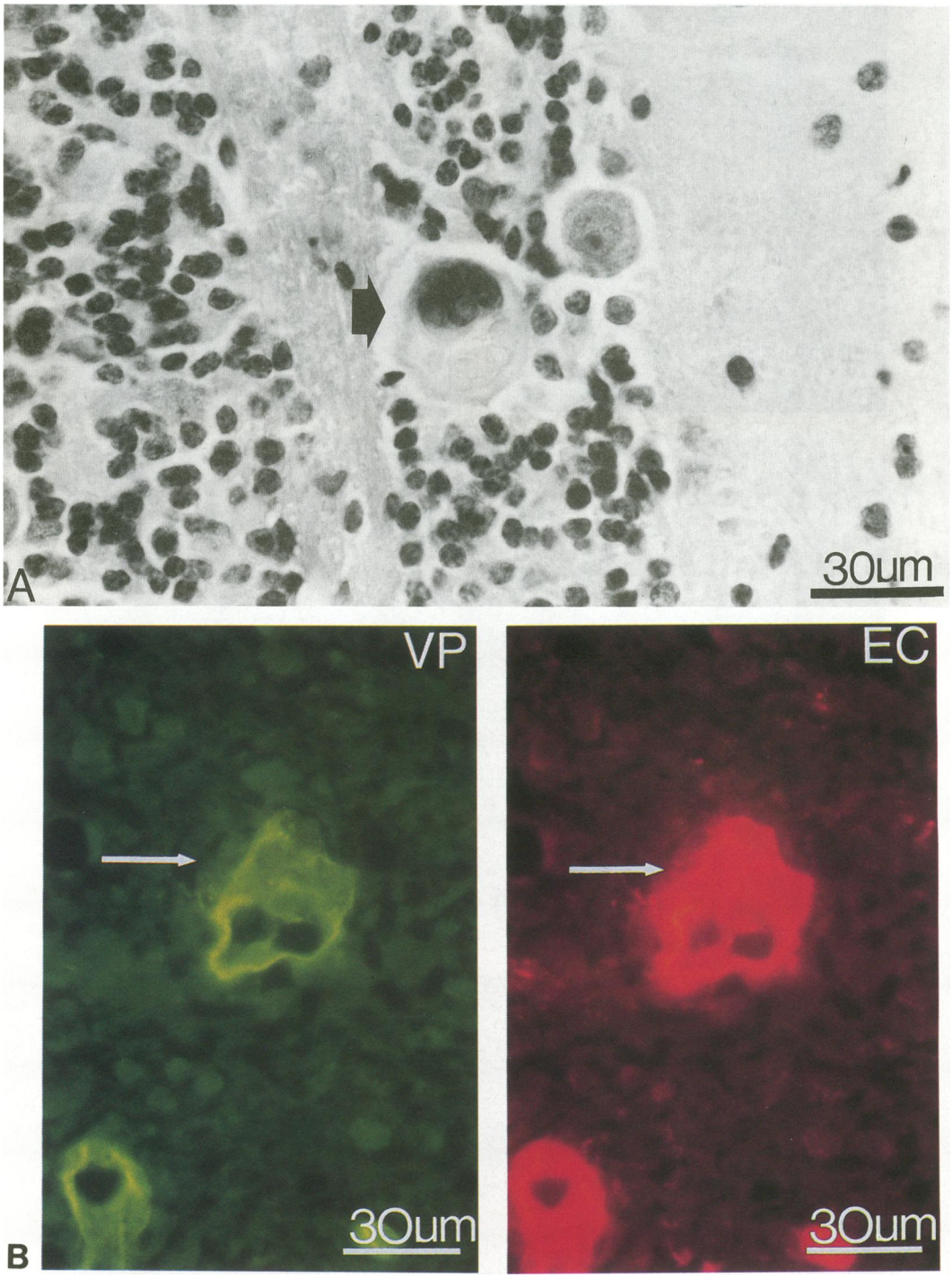

FIG. 4. Cerebral vessel endothelia form syncytia in TR1.3-infected brains. (A) High magnification of a multinucleated cerebellar vessel endothelial cell (arrow); (B) anti-Rauscher gp70 (VP)- and BS-1 lectin (EC)-double staining of a TR1.3-infected brain endothelial cell with an enlarged cytoplasm (arrows); (C) electron micrograph of a multinucleated brain endothelial cell from a TR1.3-infected mouse.

mice. These mice uniformly developed neurologic symptoms identical to those described for primary TR1.3 recipients and died within 2 weeks postinoculation. Areas of intracerebral hemorrhage and syncytium formation of endothelial cells were seen upon autopsy, and immunohistochemical analysis revealed viral infection of vessel endothelial cells, as described previously (data not shown).

Genetic homology of TR1.3 and FMuLVs. Although the pathologic effects of TR1.3 are unlike those of any previously described MuLV, infection of vessel endothelial cells has been previously observed with several MuLVs. This is most evident in members of the FMuLV family (25). In view of this observation, we evaluated the molecular homology of TR1.3 to the endothelial cell tropic FMuLV clone FB29.

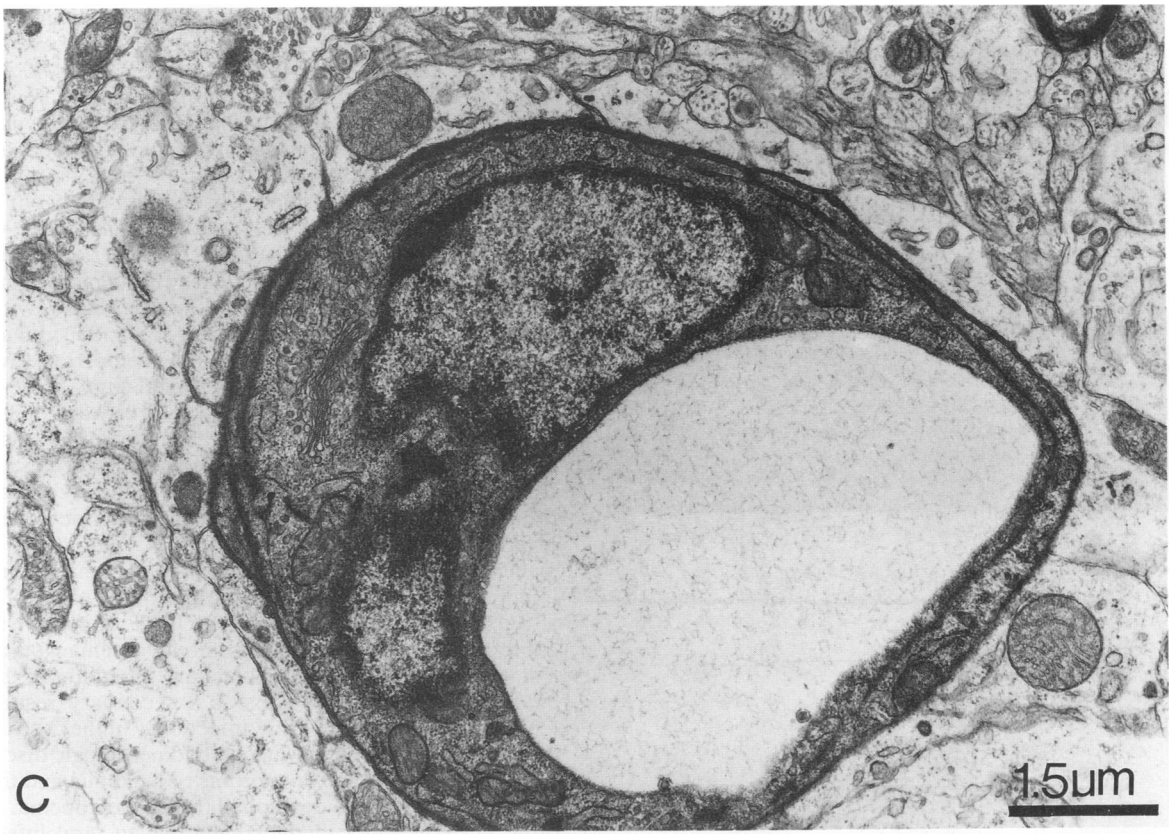

Plasmid DNAs of FB29 and TR1.3 were digested with a panel of restriction enzymes, and fragments were analyzed by gel electrophoresis. As shown in Fig. 5A, treatment of viral plasmids with the restriction enzymes *Asc*I, *Cla*I, *Eco*RI, *Hin*dIII, *Kpn*I, *Pst*I, *Pvu*II, *Nco*I, *Sph*I, and *Xba*I yielded restriction fragments of identical sizes. However, there was an additional *Hin*cII site within the *env* region of TR1.3 that was not present in the FB29 genome and a *Sac*II site within the LTR region of FB29 that was absent in the TR1.3 genome. The presence of the *Hin*cII site in TR1.3 is demarcated by the detection of new fragments at 6,000 and 4,500 bp, while the additional *Sac*II site in FB29 is demarcated by a small, poorly visible 650-bp fragment. A linear restriction map was generated from these data and is presented in Fig. 5B. These results indicate that the molecular clones TR1.3 and FB29 have similarity throughout their genomes and suggest that the TR1.3 virus is a member of the FMuLV family.

Genetic mapping of TR1.3-induced pathogenicity. To define the genomic regions of TR1.3 that are responsible for its pathogenicity, recombinant viral genomes were constructed between TR1.3 and the nonneuropathogenic FMuLV, FB29. A 3.0-kb fragment containing the 3′ end of the *pol* gene, the *env* gene, and the U3 region of the LTR was reciprocally switched between FB29 and TR1.3. As shown in Fig. 6, this dramatically affected the neuropathogenic potential of these viruses. The introduction of this 3.0-kb fragment from TR1.3 into the FB29 background produced a recombinant virus, termed R3.5, with the same disease specificity as the parental TR1.3 virus. Neonatal BALB/c mice inoculated with R3.5 uniformly exhibited neurologic symptoms of tremor, seizure, and paralysis 2 weeks postinoculation. Immunofluorescence analysis demonstrated viral infection of vessel endothelium, and histologic examination revealed hemorrhagic lesions and syncytium formation of endothelial cells (data not shown). Conversely, the neuropathogenicity of TR1.3 was completely abrogated when the 3.0-kb fragment from FB29 was introduced into the TR1.3 background (recombinant virus R4.3). The recombinant virus R4.3 infected vessel endothelial cells to equivalent levels as judged by immunofluorescence and did not induce pathologic changes in a manner identical to that of FB29 FMuLV. These data demonstrate that the unique neuropathogenicity of TR1.3 resides within this 3.0-kb fragment.

DISCUSSION

Endothelial cells play an important role in maintaining normal physiologic homeostasis. They provide a selective barrier between blood and tissues and a nonthrombogenic surface to prevent platelet adherence, and they contribute to other processes such as lymphocyte migration and inflammatory responses (10). Damage to endothelia has been shown to increase vessel permeability and has been postulated as an initiating event that leads to vascular diseases, such as atherosclerosis and stroke (5). The role of virus infection in inducing vascular disease via endothelial cell injury has remained a subject of speculation (2, 9, 38). Results described here present a retroviral system in which neurodegenerative changes can be directly attributed to endothelial cell infection by virus. Double fluorescence immunostaining indicated that the TR1.3 MuLV specifically

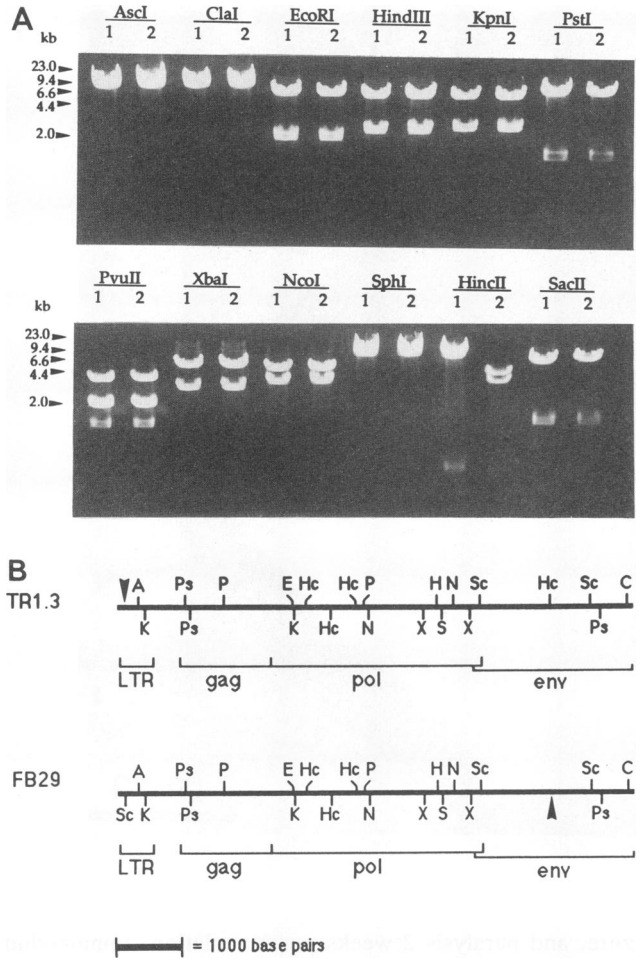

FIG. 5. Restriction fragment map of TR1.3 and FB29 MuLV. (A) Analysis of restriction fragment size and number. One microgram of FB29 plasmid DNA (lanes 1) or TR1.3 plasmid DNA (lanes 2) was incubated with the following enzymes: *Asc*I, *Cla*I, *Eco*RI, *Hin*dIII, *Kpn*I, *Pst*I (upper panel), *Pvu*II, *Nco*I, *Sph*I, *Xba*I, *Hin*cII, and *Sac*II (lower panel). Digestions were performed at 37°C for 1.5 h. Digested fragments were separated by gel electrophoresis (0.6% agarose) and stained with ethidium bromide (5 μg/ml). (B) Restriction enzyme maps of linear FB29 and TR1.3 MuLV. Arrows indicate the absence of *Hin*cII and *Sac*II restriction sites in FB29 and TR1.3, respectively. The linear maps of restriction enzyme sites were generated by using the data shown in panel A. Abbreviations: A, *Asc*I; C, *Cla*I; E, *Eco*RI; H, *Hin*dIII; K, *Kpn*I; Ps, *Pst*I; P, *Pvu*II; N, *Nco*I; S, *Sph*I; X, *Xba*I; Hc, *Hin*cII; Sc, *Sac*II.

infected vessel endothelial cells. Gross and histopathological analyses of brains from these mice demonstrated that the normal physiological function of the infected endothelial cells was compromised, resulting in acute cerebral hemorrhage and death.

A number of MuLVs infect brain CEC. These include several neuropathogenic MuLVs and nonneuropathogenic members of the FMuLV family (20, 23, 25). In each instance, these viruses have no direct effect on gross morphology or function of CEC, even though they may induce substantial changes in the function of other CNS cells. Preliminary studies in our laboratory indicate that several FMuLVs that appear to be closely related to TR1.3 yield a nonpathogenic, persistent infection of brain CEC. The demonstration that infection of CEC can occur in the absence of neuropathology strongly suggests that tropism and virulence are differentially regulated in these MuLVs. In the case of TR1.3, with which both infection and degeneration of vessel endothelial cells are observed, it is likely that CEC tropism is necessary but not sufficient to induce cytopathologic effects and subsequent neurologic disease.

Perhaps the most striking observation from our current studies is the endothelial cell pathology associated with the acute hemorrhagic response to TR1.3 infection. Portis et al. (26) have previously described a MuLV molecular clone, derived from a paralytogenic wild-mouse MuLV, with which a similar type of cranial hemorrhage was induced in only 4% of inoculated mice. In this infection, hemorrhage was confined to the hindbrains and rostral spinal cords of the affected mice. Infection of brain CEC by this virus was not assessed, although this virus did induce other types of neurodegenerative changes, e.g., spongiform encephalopathies, without CNS bleeding. These authors have suggested that some MuLV infections are associated with thrombocytopenia that could secondarily lead to cranial bleeding (26). Several pieces of evidence argue against this explanation in TR1.3 infection. The TR1.3 virus induced a quick onset of disease and exclusive cranial bleeding in 100% of mice tested. In contrast, MuLV-associated thrombocytopenia would lead to a state of systemic vascular bleeding. In addition, thrombocytopenia normally develops as a secondary result of the leukemias induced by MuLV infections. In the case of TR1.3 infection, however, mice succumb to neurologic disease well before they exhibit any symptoms of leukemia and therefore were unlikely to have developed thrombocytopenia. Finally, other systems of i.c. hemorrhage due to viral infection of brain CEC have been reported. A rat parvovirus that infects brain CEC and leads to a hemorrhagic encephalopathy has been described (7). More recently, two mouse systems of i.c. hemorrhagic lesions using MuLV pseudotyped with murine sarcoma viruses have been reported (14, 24). In these two systems, i.c. hemorrhagic lesions were associated with hemangiomas of endothelial cells. Taken together, these data suggest that structural damage to brain CEC can lead to a final degenerative pathology of i.c. hemorrhages. In the case of the TR1.3 MuLV, infection results in syncytium formation of brain CEC, leading to CEC dysfunction, i.c. bleeding, and death.

The results presented in Fig. 4 demonstrate that the formation of multinucleated endothelial cells following infection with TR1.3 is the result of syncytium formation as opposed to either endothelial cell proliferation or hemangioma formation as reported by others (14, 24). The major reason for this distinction is that there was no evidence of separation between cytoplasmic borders within these multinucleated structures, unlike with endothelial cell proliferation, which maintains cell border integrity. Electron microscopy also supports the observation of multinucleated cells, as many features of endothelial cell proliferation were absent. There was no evidence of mass or sheet-like growth, there were no dysplasia or anaplastic changes in cell nuclei, and there was no evidence of mitotic activity within these endothelial cells. Moreover, the changes in infected endothelial cells appeared to be of a degenerative nature. There were various stages of cell death in single endothelial cells, including pyknotic nuclei, karyorrhexis, and complete disintegration and necrosis.

It is clear that MuLV and other retroviruses are capable of inducing syncytia in vitro (16); however, syncytium formation in vivo by a MuLV has not previously been reported.

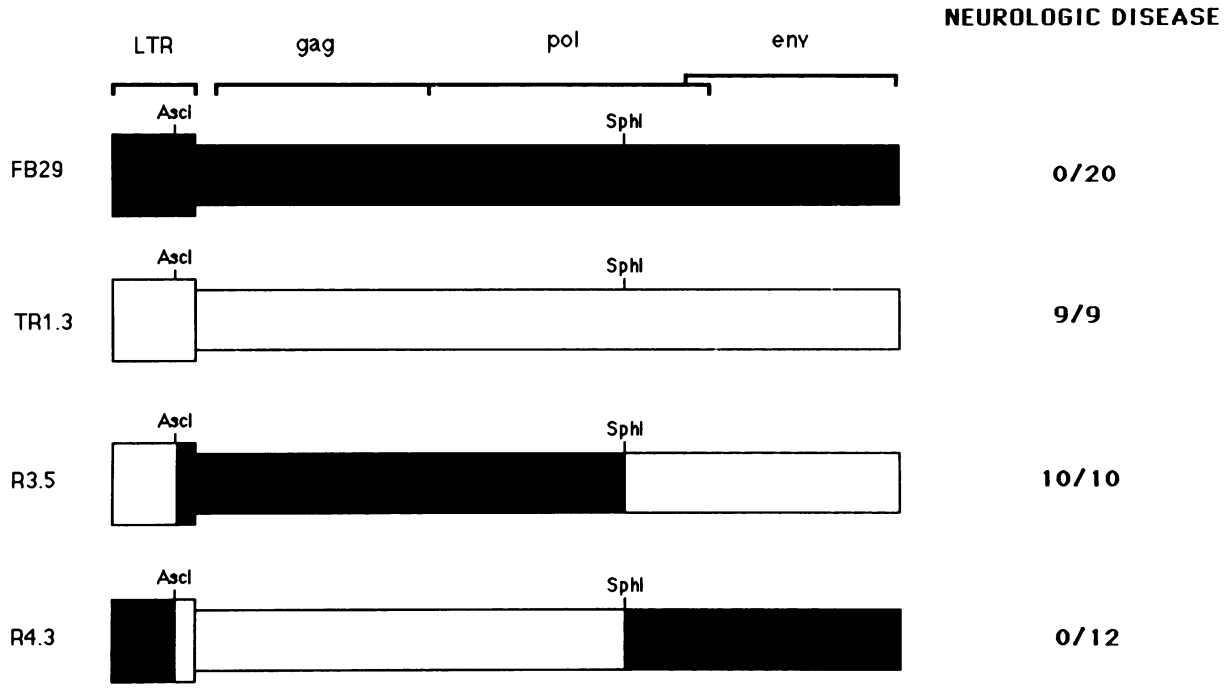

FIG. 6. Neuropathogenicity of TR1.3 resides within a 3.0-kb *Sph*I-*Asc*I fragment. Recombinant viruses were constructed from TR1.3 and FB29 in the vector pUC19B, and infectious virus was produced and used to inoculate neonatal BALB/c mice as described in Materials and Methods. Results (numbers of diseased mice from each treatment group) shown to the right are pooled from three separate experiments.

Research interest in syncytium formation has been heightened recently in an attempt to elucidate the mechanisms of human immunodeficiency virus type 1-induced syncytia of macrophages (4). Interestingly, vessel endothelia outside the brain do not form syncytia in TR1.3-infected BALB/c mice. These results suggest that there is a unique feature of brain endothelium that allows the formation of syncytia by TR1.3 MuLV. Recent reports indicate that cell-specific glycosylases may regulate in vitro syncytium formation of NIH 3T3 and XC cells (16), and we are currently addressing these possibilities for TR1.3 infection.

A key component to a mechanistic interpretation of these results lies in molecular definition of the TR1.3 virus. The results presented in Fig. 6 illustrate the widespread molecular similarity between TR1.3 and the FB29 clone of FMuLV. This is further supported by recent evidence that the *env* gene sequences of FMuLV and E55+ (TR1.3) are highly homologous (36). By constructing recombinant viruses with these two related MuLVs, the pathogenicity of TR1.3 has been localized to a 3.0-kb fragment containing the 3′ *pol* gene, the *env* gene, and the U3 portion of the LTR. The mechanism of the selective degenerative effect of TR1.3 in cerebral endothelial cells is presently unknown. Neurotropism and virulence have been mapped to the *env* and LTR regions of other MuLVs (6, 21, 22). For example, Masuda et al. (20) have shown that a primary determinant of neurovirulence is found within the *env* gene of an FMuLV variant. Small changes within these regions can dramatically affect virus virulence. Szurek et al. (35) have reported that a single amino acid substitution in the *env* gene of the nonneuropathic Moloney MuLV results in the neurovirulent temperature-sensitive mutant, *ts*1. It is, therefore, possible that subtle changes in the *env* gene with respect to FMuLV confer the neuropathogenic potential of TR1.3.

Viral tropism and virulence may also be regulated at the RNA level through the selective activation of the LTR. The LTR modulates viral transcription through binding of specific nuclear factors present within the host cell (19). This suggests the possibility that unique binding proteins within brain CEC activate the LTR, allowing the production of viral RNA in a tissue-specific manner. In this regard, brain CEC demonstrate a number of differences compared with CEC found elsewhere in the body, including the formation of tight junctions, lack of vesiculation, and alkaline phosphatase activity (reviewed in reference 1). Studies are presently under way to further define the genomic regions that mediate TR1.3 tropism and neurovirulence.

In summary, infectious virus was produced from a molecular clone derived from a T-cell tropic MuLV. Inoculation of this virus into neonatal BALB/c mice uniformly induced an acute onset of cranial hemorrhage, neurologic symptoms, and death. Because of its similarity with the nonneuropathic FMuLV, the TR1.3 virus provides a powerful model for dissecting the molecular parameters involved in inducing this unique form of retrovirus-associated neurologic disease.

ACKNOWLEDGMENTS

We thank John Portis for the FB29 clone, Anna Stieber for technical assistance, Frank Burns for technical guidance, and Peter Williamson for critical review of the manuscript.

B.H.P. is an MSTP fellow, supported by grant 5-T32-GM-07170. G.N.G. is a scholar of the Leukemia Society of America. This work was supported by grant PO1-NS30606.

REFERENCES

1. **Beilke, M. A.** 1989. Vascular endothelium in immunology and infectious disease. Rev. Infect. Dis. **11**:273–283.
2. **Benditt, E. P., T. Barrett, and J. K. McDougall.** 1983. Viruses in

the etiology of atherosclerosis. Proc. Natl. Acad. Sci. USA **80**:6386–6389.
3. **Carneiro, A. V., J. Ferro, C. Figueiredo, L. Costa, J. Campos, and F. dePadua.** 1991. Herpes zoster and contralateral hemiplegia in one African patient infected with HIV-1. Acta. Med. Port. **4**:91–92.
4. **Chowdhury, M. I., Y. Koyanagi, M. Suzuki, S. Kobayashi, K. Yamaguchi, and N. Yamamoto.** 1992. Increased production of human immunodeficiency virus (HIV) in HIV-induced syncytia formation: an efficient infection process. Virus Genes **6**:63–78.
5. **Cotran, R. S., V. Kumar, and S. L. Robbins.** 1989. Robbins pathologic basis of disease, 4th ed., p. 553–596. W. B. Saunders Company, Harcourt Brace Jovanovich, Inc., Philadelphia.
6. **DesGroseillers, L., E. Rassart, Y. Robitaille, and P. Jolicoeur.** 1985. Retrovirus-induced spongiform encephalopathy: the 3′-end long terminal repeat-containing viral sequences influence the incidence of the disease and the specificity of the neurologic syndrome. Proc. Natl. Acad. Sci. USA **82**:8818–8822.
7. **El Dadah, A. H., N. Nathanson, K. O. Smith, R. A. Squire, G. W. Santos, and E. C. Melby.** 1967. Viral hemorrhagic encephalopathy of rats. Science **156**:392–394.
8. **Engstrom, J. W., D. H. Lowenstein, and D. E. Bredesen.** 1989. Cerebral infarctions and transient neurologic deficits associated with acquired immunodeficiency syndrome. Am. J. Med. **86**: 528–532.
9. **Fabricant, C. G.** 1985. Atherosclerosis: the consequence of infection with a herpesvirus. Adv. Vet. Sci. Comp. Med. **30**:39–66.
10. **Friedman, H. M., E. J. Macarak, R. R. MacGregor, J. Wolfe, and N. Kefalides.** 1981. Virus infection of endothelial cells. J. Infect. Dis. **143**:266–273.
11. **Gardner, M. B.** 1985. Retroviral spongiform polioencephalomyelopathy. Rev. Infect. Dis. **7**:99–110.
12. **Goff, S., P. Traktman, and D. Baltimore.** 1981. Isolation and properties of Moloney murine leukemia virus mutants. Use of a rapid assay for the release of virion reverse transcriptase. J. Virol. **38**:238–248.
13. **Hashimoto, Y., and K. J. Blank.** 1990. T cell receptor genes and T cell development in virus-transformed early T cell lines. J. Immunol. **144**:1518–1525.
14. **Hevezi, P., and S. P. Goff.** 1991. Generation of recombinant murine retroviral genomes containing the v-*src* oncogene: isolation of a virus inducing hemangiosarcomas in the brain. J. Virol. **65**:5333–5341.
15. **Hirt, B.** 1967. Selective extraction of polyoma DNA from infected mouse cell cultures. J. Mol. Biol. **26**:365–369.
16. **Jones, J. S., and R. Risser.** 1993. Cell fusion induced by the murine leukemia virus envelope glycoprotein. J. Virol. **67**:67–74.
17. **Laitinen, L.** 1987. Griffonia simplicifolia lectins bind specifically to endothelial cells and some epithelial cells in mouse tissues. Histochem. J. **19**:225–234.
18. **Lynch, W. P., S. Czub, F. J. McAtee, S. F. Hayes, and J. L. Portis.** 1991. Murine retrovirus-induced spongiform encephalopathy: productive infection of microglia and cerebellar neurons in accelerated CNS disease. Neuron **7**:365–379.
19. **Manley, N. R., M. A. O'Connell, P. A. Sharp, and N. Hopkins.** 1989. Nuclear factors that bind to the enhancer region of nondefective Friend murine leukemia virus. J. Virol. **63**:4210–4223.
20. **Masuda, M., M. P. Remington, P. M. Hoffman, and S. K. Ruscetti.** 1992. Molecular characterization of a neuropathogenic and nonerythroleukemogenic variant of Friend murine leukemia virus PVC-211. J. Virol. **66**:2798–2806.
21. **Paquette, Y., Z. Hanna, P. Savard, R. Brousseau, Y. Robitaille, and P. Jolicoeur.** 1989. Retrovirus-induced murine motor neuron disease: mapping the determinant of spongiform degeneration within the envelope gene. Proc. Natl. Acad. Sci. USA **86**:3896–3900.
22. **Paquette, Y., D. G. Kay, E. Rassart, Y. Robitaille, and P. Jolicoeur.** 1990. Substitution of the U3 long terminal repeat region of the neurotropic Cas-Br-E retrovirus affects its disease-inducing potential. J. Virol. **64**:3742–3752.
23. **Pitts, O. M., J. M. Powers, J. A. Bilello, and P. M. Hoffman.** 1987. Ultrastructural changes associated with retroviral replication in central nervous system capillary endothelial cells. Lab. Invest. **56**:401–409.
24. **Pitts, O. M., J. M. Powers, and P. M. Hoffman.** 1983. Vascular neoplasms induced in rodent central nervous system by murine sarcoma viruses. Lab. Invest. **49**:171–182.
25. **Portis, J. L.** 1990. Wild mouse retrovirus: pathogenesis. Curr. Top. Microbiol. Immunol. **160**:11–27.
26. **Portis, J. L., S. Czub, C. F. Garon, and F. J. McAtee.** 1990. Neurodegenerative disease induced by the wild mouse ecotropic retrovirus is markedly accelerated by long terminal repeat and *gag-pol* sequences from nondefective Friend murine leukemia virus. J. Virol. **64**:1648–1656.
27. **Rawlinson, W. D., and A. L. Cunningham.** 1991. Contralateral hemiplegia following thoracic Herpes zoster. Med. J. Aust. **155**:344–346.
28. **Ross, R.** 1986. The pathogenesis of atherosclerosis—an update. N. Engl. J. Med. **314**:488–500.
29. **Rowe, W. P., W. E. Pugh, and J. W. Hartley.** 1970. Plaque assay techniques for murine leukemia viruses. Virology **42**:1136–1139.
30. **Scaravilli, F., S. E. Daniel, N. Harcourt-Webster, and R. J. Guiloff.** 1989. Chronic basal meningitis and vasculitis in acquired immunodeficiency syndrome. Arch. Pathol. Lab. Med. **113**:192–195.
31. **Sharpe, A. H., J. J. Hunter, P. Chassler, and R. Jaenisch.** 1990. Role of abortive retroviral infection of neurons in spongiform CNS degeneration. Nature (London) **346**:181–183.
32. **Shuper, A., E. P. Vining, and J. M. Freeman.** 1990. Central nervous system vasculitis after chicken pox: cause or coincidence. Arch. Dis. Child. **65**:1245–1248.
33. **Simonian, N. A., L. A. Rosenthal, J. Korostoff, W. F. Hickey, K. J. Blank, and G. N. Gaulton.** 1990. Specific infection of central nervous system white matter by a variant of Gross murine leukemia virus. Virology **177**:384–387.
34. **Sitbon, M., B. Sola, L. Evans, J. Nishio, S. F. Hayes, K. Nathanson, C. F. Garon, and B. Chesebro.** 1986. Hemolytic anemia and erythroleukemia, two distinct pathogenic effects of Friend MuLV: mapping of the effects to different regions of the viral genome. Cell **47**:851–859.
35. **Szurek, P. F., P. H. Yuen, J. K. Ball, and P. K. Y. Wong.** 1990. A Val-25-to-Ile substitution in the envelope precursor polyprotein, $gPr80^{env}$, is responsible for the temperature sensitivity, inefficient processing of $gPr80^{env}$, and neurovirulence of *ts*1, a mutant of Moloney murine leukemia virus TB. J. Virol. **64**:467–475.
36. **Tumas, K. M., J. M. Poszgay, N. Avidan, S. Ksiazek, B. Overmoyer, K. J. Blank, and M. B. Prystowsky.** 1992. Loss of antigenic epitopes as the result of env gene recombination in retrovirus-induced leukemia in immunocompetent mice. Virology **192**:587–595.
37. **Wigler, M., A. Pellicer, S. Silverstein, R. Axel, G. Urlaub, and L. Chasin.** 1979. DNA-mediated transfer of the adenine phosphoribosyltransferase locus into mammalian cells. Proc. Natl. Acad. Sci. USA **76**:1373–1376.
38. **Wiley, C. A., R. D. Schrier, J. A. Nelson, P. W. Lampert, and M. B. A. Oldstone.** 1986. Cellular localization of human immunodeficiency virus infection within the brains of acquired immune deficiency syndrome patients. Proc. Natl. Acad. Sci. USA **83**:7089–7093.